CHINESE OPTICS LETTERS

Vol. 22, No. 3 | March 2024

Power output correction model of narrow linewidth ring fiber laser filtered with whispering gallery mode resonator

Ziyun Wang (王子云)[1,2], Zaibin Xu (徐在斌)[1,2], Jiwen Cui (崔继文)[1,2*], and Jiubin Tan (谭久彬)[1,2]

[1] Center of Ultra-precision Optoelectronic Instrument, Harbin Institute of Technology, Harbin 150080, China

[2] Key Laboratory of Ultra-precision Intelligent Instrumentation, Ministry of Industry and Information Technology, Harbin Institute of Technology, Harbin 150080, China

*Corresponding author: cuijiwen@hit.edu.cn

Received October 3, 2023 | Accepted October 27, 2023 | Posted Online March 19, 2024

A whispering gallery mode resonator (WGMR) filter can narrow laser linewidth while significantly changing the output power characteristics of fiber laser system. It is found that traditional laser output power model is invalid. We report a correction model of a narrow linewidth fiber laser filtered with a WGMR to analyze its power. We believe that the loss of the laser system and the threshold gain increase caused by the WGMR filter lead to the predominate amplified spontaneous emission during the original laser period. According to that, we assume the correction coefficient is an exponential decay related to the Er-doped fiber length in the large loss situation, and we verify it experimentally. As a result, the correction model is valid for WGMR-filtered fiber laser.

Keywords: whispering gallery resonator filter; narrow linewidth fiber laser; power output correction model.
DOI: 10.3788/COL202422.031401

1. Introduction

Fiber lasers have the advantage of having a narrow linewidth, low noise[1], and an all fiber structure and are widely used in distributed fiber sensing[2], high-resolution coherent spectral analysis[3], coherent optical communication, and other fields[4]. The narrow linewidth performance of lasers is required in the fields above, and in fiber optic sensing technologies such as optical frequency domain reflection (OFDR) technology and phase-sensitive optical time-domain reflection (φ-OTDR) technology. In recent years, with the development of fiber technology and new photonic devices, fiber lasers have made rapid progress. Filter devices such as Fabry–Perot cavities and fiber gratings are often used to achieve mode selection and narrow linewidth of fiber lasers. In theory, compared with these filters, the whispering gallery mode resonator (WGMR) has a higher Q (typical value 10^8), narrower transmission bandwidth, and great linewidth narrowing capability[5].

In recent years, with the development of precision machining technology, it is common to produce WGMRs[6,7] with a Q of up to 10^8 or even 10^9. With its ultra narrow resonant peak transmission spectrum, the laser linewidth can be obviously compressed. Taking 10^8 Q as an example, its corresponding resonant peak bandwidth of the WGMR is in MHz, and only the optical frequency in the resonant spectra of the WGMRs can enter into the WGMRs. Then, the light excites reverse Rayleigh scattering[8,9] and circulates inside the ring fiber laser cavity. The process above realizes the linewidth narrowing. Therefore, WGMRs are narrowband filters equivalently.

In 2007, Kieu and Mansuripur first reported a fiber laser structure with a microsphere WGMR as the feedback element[10]. This structure has a Q factor of 10^8 which corresponds to a filter bandwidth of MHz. Its reverse Rayleigh scattering light is used as the feedback signal, and the laser linewidth is less than 100 kHz. In 2013, River-Pérez *et al.* reported a ring fiber laser structure using a microsphere WGMR as a narrowband filter[11]. It was tunable by tuning the resonant peaks of the WGMR. Its laser linewidth was less than 35 kHz, the power was 0.38 mW, and the tuning range was 1.16 nm. In 2018, Huang *et al.*, in order to broaden the tuning range of the laser, used a microsphere WGMR and fiber grating to construct frequency selectors, adjusted the center frequency of the fiber grating through stress, selected different mode resonant peaks to form a single-mode resonance, and realized the laser frequency shift. The tuning range was 30 nm, and the linewidth was 5 kHz. At the same time, using the thermo optic effect of the microcavity, its resonant peak could be moved slightly in the FBG bandwidth range, realizing the fine tuning of the laser[12]. In 2018, Ma *et al.* constructed a fiber laser system by using the microbottle cavity as a filter and tuning device[13]. This scheme coated some surfaces of the microbottle cavity with iron oxide particles and introduced controlled light along the axis of the microcapsule cavity. Using the photothermal effect of the surface iron oxide

to change the size and refractive index of the microcapsule cavity, all optical tuning was achieved by changing the power of the control light. The tuning range was 2.7 nm, the linewidth was 500 Hz, and the scheme required the pump source power to be less than 180 mW. Otherwise, it would cause the stimulated radiation of the suppressed higher-order modes, leading to a multimode output. Therefore, the laser output power was only 4 μW.

At present, fiber laser structures filtered with a WGMR have broad development prospects and application requirement. However, there are also some problems, such as low laser output power (in most cases it is only μW level). To the best of our knowledge, there are few reports analyzing the power characteristics of the WGMR-filtered fiber lasers. The traditional fiber laser power analysis model has been widely adopted and obtained results consistent with experimental results[14,15]. However, when we used the model to analyze the output power of the WGMR-filtered fiber laser, there is a difference of three orders from the experimental results, indicating that the traditional model cannot accurately analyze the power output of the WGMR-filtered fiber laser. Therefore, based on the available theory, we establish a power output correction model of the WGMR-filtered fiber laser and conduct numerical simulations, which agree well with experimental results and verify the correction model.

2. Power Output Correction Model of the WGMR-filtered fiber Laser

The schematic diagram of the traditional ring fiber laser is shown in Fig. 1(a). The traditional power model is introduced next. Based on the energy level rate equation of the doped fiber (erbium-doped fiber in this paper), Eq. (1), the fiber output equation such as Eqs. (2) and (3), and the boundary conditions of the ring resonator, the laser output power, $P_s(z)$, can be calculated as Eq. (4).

$$\frac{\mathrm{d}N_2(z,t)}{\mathrm{d}t} = \left[\frac{\sigma_a\Gamma_s}{h\nu_s A}P_s(z) + \frac{\sigma_p\Gamma_p}{h\nu_p A}P_P(z)\right]N_1(z,t) - \frac{\sigma_e\Gamma_s}{h\nu_s A}P_s(z)N_2(z,t) - A_{21}N_2(z,t), \tag{1}$$

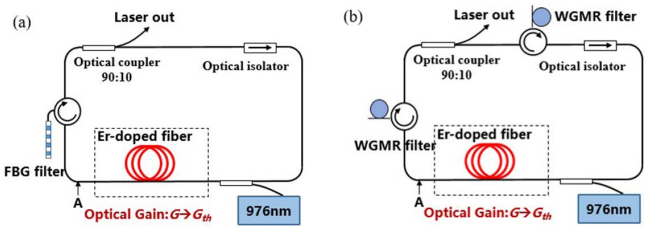

Fig. 1. Schematic diagram of the fiber laser structure. (a) The common ring fiber laser structure uses FBG filters to achieve single mode operation. (b) The ring fiber laser filtered with WGMR.

$$\frac{\mathrm{d}P_p(z)}{\mathrm{d}z} = -P_p(z)\Gamma_p\sigma_p N_1(z,t), \tag{2}$$

$$\frac{\mathrm{d}P_s(z)}{\mathrm{d}z} = P_s(z)\Gamma_s[\sigma_e N_2(z,t) - \sigma_a N_1(z,t)], \tag{3}$$

$$P_s(L) = \frac{\lambda_p}{\lambda_s}\frac{1-\exp\left[\frac{\Gamma_p\sigma_p}{\Gamma_s(\sigma_a+\sigma_e)}(G_{\mathrm{th}} - \Gamma_s\sigma_e N_{\mathrm{Er}}L)\right]}{1+\exp(-G_{\mathrm{th}})}(P_p^{\mathrm{in}} - P_{\mathrm{pth}}^{\mathrm{in}}). \tag{4}$$

In Eq. (1), $N_2(z)$ is the number of particles at the upper level of the erbium-doped fiber, and $N_1(z)$ is the number of particles at the lower level of the erbium-doped fiber. σ_s is the signal light absorption cross section coefficient, σ_e is the signal light radiation cross section coefficient, and σ_p is the absorption cross section coefficient of the pump light. ν_s is the optical frequency of the pump light, and ν_p is the optical frequency of the pump light. Γ_s is the overlap factor of the signal light, Γ_e is the overlap factor of the pump light, and h is the Planck constant. A is the effective area of the erbium-doped fiber core, and A_{21} is the probability of spontaneous emission of the energy level particles on the erbium-doped fiber core.

Since the amplified spontaneous emission (ASE) is far weaker than the signal light when the conventional laser reaches the steady state output, the available power model ignores the ASE effect. In the early stage of laser superfluorescence formation, the small signal gain coefficient G_0 gradually decreases with the continuous enhancement of the intracavity optical field. When G_0 decreases to the system loss, the intracavity light field no longer increases and reaches its maximum value. The G_0 remains constant, and the laser output remains stable. At this state, the gain coefficient is called threshold gain G_{th}, which is related to the laser system loss. The calculation formula is shown in Eq. (5),

$$G_{\mathrm{th}} = \delta = \mathrm{In}(k/R_0), \tag{5}$$

where k is the attenuation loss of the laser system without a filter (ratio of input to output), and R is the reflectivity of the WGMR filter. k is mainly caused by the loss of the circulator, wavelength-division multiplexing, and flange connection, k is 1.467 in the system of Figs. 1(a) and 1(b), and the filter reflectivity (R_0) of the conventional fiber laser is high (typical FBG filter reflectivity is 0.95). The reflectivity of the WGMR filter is extremely low, approximately 0.5% in this system. After calculation, the threshold gain G_{th} of the conventional fiber laser system is 0.43, and the threshold gain G_{th} of the WGMR filtered laser system in Fig. 1(b) is 3.89.

As mentioned above, compared with the traditional fiber laser, the reflectivity of the WGMR filter is so low that this laser has a large loss, which leads to the laser gain falling to the threshold value in a shorter time. The signal light has few times to be amplified repeatedly, and the power is weak. In this situation, the ASE process needs to be considered to correctly analyze the power output of the signal light[16–19]. This is also why the conventional fiber laser power model is no longer applicable.

In this paper, considering the effect of the ASE, the signal light in Eq. (1) is replaced by the sum of the signal light (P_s) and the

ASE (P_{ASE}). Equation (8) is obtained by simultaneously solving Eqs. (2), (3), (6), and (7). According to fiber laser theory, most of the upper-level particles in the Er doping fiber are used to amplify the spontaneous emission, and they are exponentially delayed, as the time, the spontaneous emission coefficient G_{th}, A_{21}, and the Er-doped fiber length L are key parameters (the amplified time maybe is related to G_{th}). Thus, it is assumed that the ASE power is a multiple of the signal light power, and the multiple is an exponential delay related to A_{21} and L, as shown in Eq. (9).

In the equation, a_1 and a_2 are undetermined parameters, which can be obtained through experimental tests.

$$\frac{\mathrm{d}N_2(z,t)}{\mathrm{d}t} = \left[\frac{\sigma_a\Gamma_s}{h\nu_s A}P_{s,\mathrm{ASE}}(z) + \frac{\sigma_p\Gamma_p}{h\nu_p A}P_P(z)\right]N_1(z,t) - \frac{\sigma_e\Gamma_s}{h\nu_s A}P_{s,\mathrm{ASE}}(z)N_2(z,t) - A_{21}N_2(z,t), \tag{6}$$

$$P_{s,\mathrm{ASE}}(z) = P_{\mathrm{ASE}}(z) + P_s(z) = [\beta(\delta)+1]P_s(z), \tag{7}$$

$$P_s(L) = \beta(\delta)\frac{\lambda_p}{\lambda_s}\frac{1-\exp\left[\frac{\Gamma_p\sigma_p}{\Gamma_s(\sigma_a+\sigma_e)}(G_{\mathrm{th}}-\Gamma_s\sigma_e N_{\mathrm{Er}}L)\right]}{1+\exp(-G_{\mathrm{th}})}(P_p^{\mathrm{in}}-P_{p\mathrm{th}}^{\mathrm{in}}), \tag{8}$$

$$\beta(\delta) = \left[\frac{1}{a_1\ \exp(a_2A_{21}L)}\right]^{\frac{G_{\mathrm{th}}}{3.89}}. \tag{9}$$

3. Experiments and Results

To obtain the key parameters of Eq. (9) and verify the correction model proposed in this paper, the structure design of a WGMR filtered ring fiber laser is conducted, as shown in Fig. 1(b), which is in the form of a ring optical path. An erbium-doped fiber (model Er110-4/125, Micro Photons Technology Shanghai Corporation) is used as the gain medium, and a 976-nm laser (Shanghai Hanyu Company) is used as the pump source. A fiber grating is connected to obtain a single longitudinal mode output, and an isolator is added to ensure the unidirectional operation of the laser. In particular, the WGMR filter used in this paper is made of a quartz material with a cylindrical structure, a diameter of 5 mm, and a Q factor of 9.02×10^8. The resonant peak bandwidth is only 0.22 MHz (developed by Peking University Yangtze Delta Institute of Optoelectronics). In order to achieve the ideal resonant peak of the WGMR, it is necessary to ensure a strict critical coupling state between the tapered fiber and the WGMR. The volume of the WGMR is small and easily affected by environmental factors such as temperature fluctuations and vibration, so it is necessary to package the cavity to ensure that the WGMR maintains a stable coupling state for a long time.

As shown in Fig. 1(b), we designed the WGMR-filtered fiber laser structure in a ring path and found that its output power was reduced by three orders of magnitude, compared with ordinary fiber lasers. Meanwhile, according to the traditional fiber laser power model, the power of the WGMR filtered laser was in the order of mW, which, as shown in Fig. 2(a), is obviously inconsistent with the experiment results in this paper. Additionally, we tested the output fluorescence spectrum of the Er-doped fiber end in the fiber laser system with and without the WGMR in Fig. 2(b). It can be seen that the ASE caused by the WGMR in the figure is obvious.

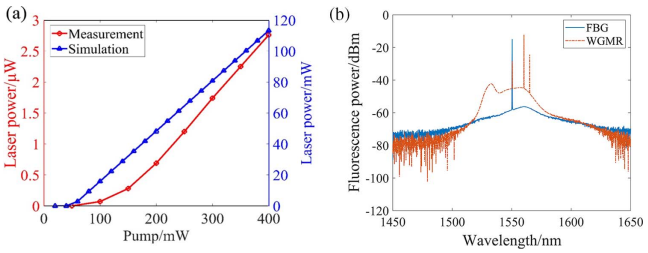

Fig. 2. Power output of a WGM filtered fiber laser at different pump powers and laser spectrum. (a) Experiment and simulation results using the traditional ring fiber laser power analysis model. (b) Output fluorescence spectrum of the Er-doped fiber end point A (as shown in Fig. 1) in the FBG and WGMR system.

The power correction model proposed in this paper is used to analyze the power output of the laser. The laser power output under different filtering losses is tested through experiments, as shown in Fig. 3(a). The parameter a_1 is 1.9×10^5 and a_2 is 0.031, both obtained using the least squares method. Based on the correction model and the parameters above, Fig. 3 shows the power output calculation of the WGMR-filtered fiber laser as optical attenuation. The simulation analysis and experiment results are basically consistent. The results indicate that the correction model is reasonable.

To further verify the correction model, the power output of the fiber laser is tested at 200 mW and 250 mW pump power, and the simulation is conducted based on the correction model and parameters above. The experiment and simulation results are shown in Fig. 4, which are basically consistent. However, compared to the case of the 300 mW pump power, there is a significant deviation between the simulation and experiment results. We believe that the correction coefficient β is related to the pump light power as well. The pump light power will increase the small signal gain of the laser. Therefore, maybe

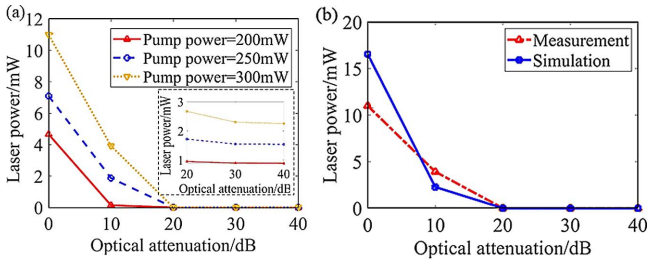

Fig. 3. (a) The output power test results of a laser with a loss of 0–40 dB at different pump powers (200 mW, 250 mW, and 300 mW). The inset in the figure shows the amplification of the 20–40 dB range. (b) The output power experiment and simulation results of a laser with a pump power of 300 mW at a loss of 0–40 dB.

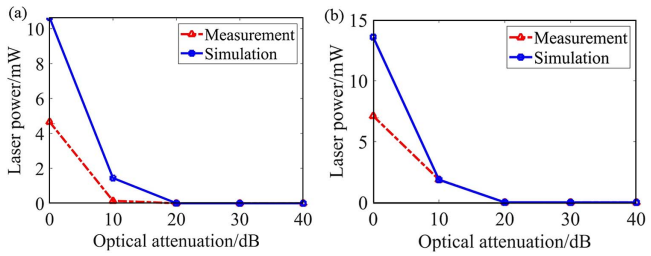

Fig. 4. (a) Comparison between the simulation results and test results of the laser power output at a pump power of 200 mW. (b) Comparison between the simulation results and test results of the laser power output at a pump power of 250 mW.

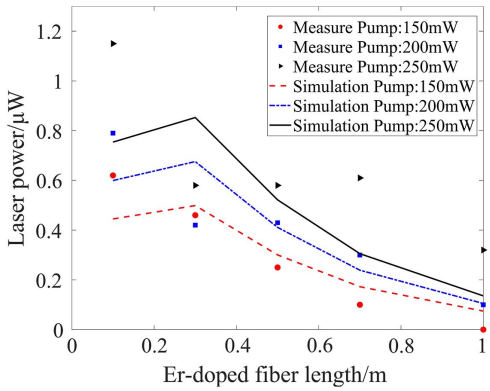

Fig. 5. Comparison between the simulation results and test results of the laser power output with different L at a pump power of 150 mW, 200 mW, and 250 mW.

the larger the pump light power, the weaker the impact of the filter loss on the power output of the laser. This guess still needs further verification experimentally and theoretically. At present, we cannot explain the deviation with certainty, and we explore this in our future research.

To adapt to the different ring fiber laser filtered with the WGMR, we construct the ring fiber laser with a different Er-doped fiber length and measure the laser output power. The improved correction model calculation essentially agrees with the test results, as shown in Fig. 5.

In particular, the WGMR is sensitive to the temperature fluctuation because of its thermo-optical and thermal expansion effects. Fortunately, the packaging process has largely been improved. The main performances of the WGMRs can remain stable in a wide temperature range. The WGMR in this paper has been tested many times (Peking University Yangtze Delta Institute of Optoelectronics, China). The results show that the Q factor only changes 2.06%, and the optical transmission only changes 2.5% relatively, when the temperature changes from −25°C to 70°C. The input power of the WGMR is generally at the mW level, and its variation should be slighter. Additionally, the stability of the WGMRs will improve further after connecting with the PID controller in future research.

4. Conclusion and Prospects

In this paper, a WGMR filtered ring fiber laser system is constructed. It is found that the available traditional fiber laser power model could not correctly analyze the power characteristics of this type of laser. This paper proposes a correction model of the WGMR-filtered fiber laser. It is believed that the unstable period of the laser process is reduced, and the significant ASE effect cannot be ignored in this process. We assume that the correction coefficient is an exponential decay related to the laser WGMR loss, and its key parameters are given by tests. The simulation results of the correction power model are basically consistent with the experimental results. During our study, we found that the WGMR filter not only changes the power output characteristics of the laser system but also changes the key parameters such as the pump threshold of the laser and the optimal length of the doped fiber. This is also the focus of our subsequent research. In addition, it is necessary to continue to study the influence of the ASE on the signal optical gain characteristics in the unstable process of the fiber lasers with large filter loss. This work and our upcoming research have important guiding significance for the design of WGMR-filtered fiber lasers.

Acknowledgements

This work was supported by the National Natural Science Foundation of China (NSFC) (No. 52075131).

References

1. S. Fu, W. Shi, Y. Feng, *et al.*, "Review of recent progress on single-frequency fiber lasers [Invited]," J. Opt. Soc. Am. B **34**, A49 (2017).
2. G. Yin, L. Lu, L. Zhou, *et al.*, "Distributed directional torsion sensing based on an optical frequency domain reflectometer and a helical multicore fiber," Opt. Express **28**, 16140 (2020).
3. K. Feng, J. Cui, H. Dang, *et al.*, "Investigation and development of a high spectral resolution coherent optical spectrum analysis system," Opt. Express **24**, 25389 (2016).
4. E. Agrell, M. Karlsson, A. R. Chraplyvy, *et al.*, "Roadmap of optical communications," J. Opt. **18**, 063002 (2016).
5. H. Wan, H. Li, H. Zhu, *et al.*, "Tunable, ultra-narrow-band optical filter based on a whispering gallery mode hybrid-microsphere," Chin. Opt. Lett. **14**, 112302 (2016).
6. G. Lin, R. Henriet, A. Coillet, *et al.*, "Dependence of quality factor on surface roughness in crystalline whispering-gallery mode resonators," Opt. Lett. **43**, 495 (2018).
7. J. Gu, J. Liu, Z. Bai, *et al.*, "Dry-etched ultrahigh-Q silica microdisk resonators on a silicon chip," Photonics Res. **9**, 722 (2021).
8. T. J. Kippenberg, S. M. Spillane, and K. J. Vahala, "Modal coupling in traveling-wave resonators," Opt. Lett. **27**, 1669 (2002).
9. M. L. Gorodetsky and V. S. Ilchenko, "Optical microsphere resonators: optimal coupling to high-Q whispering-gallery modes," J. Opt. Soc. Am. B **16**, 147 (1999).
10. K. Kieu and M. Mansuripur, "Fiber laser using a microsphere resonator as a feedback element," Opt. Lett. **32**, 244 (2007).
11. E. Rivera-Pérez, A. Díez, M. V. Andrés, *et al.*, "Tunable narrowband fiber laser with feedback based on whispering gallery mode resonances of a cylindrical microresonator," Opt. Lett. **38**, 1636 (2013).
12. L. Huang, P. Chang, X. Li, *et al.*, "All-fiber narrow-linewidth ring laser with continuous and large tuning range based on microsphere resonator and fiber Bragg grating," Opt. Express **26**, 32652 (2018).

13. R. Ma, S. Yuan, S. Zhu, *et al.*, "Tunable sub-kHz single-mode fiber laser based on a hybrid microbottle resonator," Opt. Lett. **43**, 5315 (2018).
14. C. Barnard, P. Myslinski, and M. Kavehrad, "Analytical model for rare-earth-doped fiber amplifiers and lasers," IEEE J. Quantum Electron. **30**, 1817 (1994).
15. T. Pfeiffer, H. Schmuck, and H. Bulow, "Output power characteristics of erbium-doped fiber ring lasers," IEEE Photon. Technol. Lett. **4**, 847 (1992).
16. G. J. Linford, E. R. Peressini, W. R. Sooy, *et al.*, "Very long lasers," Appl. Opt. **13**, 379 (1974).
17. E. Desurvire and J. R. Simpson, "Amplification of spontaneous emission in erbium-doped single-mode fibers," J. Lightwave Technol. **7**, 835 (1989).
18. O. Svelto, S. Taccheo, and C. Svelto, "Analysis of amplified spontaneous emission: some corrections to the Linford formula," Opt. Commun. **149**, 277 (1998).
19. G. G. Moghadam and A. H. Farahbod, "General formula for calculation of amplified spontaneous emission intensity," Opt. Quantum Electron. **48**, 277 (2016).